Am J Cancer Res 2024;14(12):5697-5716
www.ajcr.us /ISSN:2156-6976/ajcr0161065

Original Article

Blockade of neutral sphingomyelinase 2 exerts antitumor effect on metastatic castration resistant prostate cancer cells and promotes tumor regression when combined with Enzalutamide

Shams GE Shams[1*], Dalal Dawud[1*], Kasia Michalak[1], Maysoon M Makhlouf[1], Ahmed Moustafa[2], S Michal Jazwinski[2], Lin Kang[1,4,5], Mourad Zerfaoui[3], Khalid A El Sayed[4], Zakaria Y Abd Elmageed[1,4]

[1]Department of Biomedical Sciences, Discipline of Pharmacology, Edward Via College of Osteopathic Medicine (VCOM), Monroe, LA 71203, USA; [2]Tulane Center for Aging, School of Medicine, Tulane University, New Orleans, LA 70112, USA; [3]Department of Pediatrics, Center for ViroScience and Cure (CVC), School of Medicine, Emory University, Atlanta, GA 30322, USA; [4]School of Basic Pharmaceutical and Toxicological Sciences, College of Pharmacy, University of Louisiana at Monroe, Monroe, LA 71201, USA; [5]Center for One Health Research, VA-MD College of Veterinary Medicine, Blacksburg, VA 24060, USA. [*]Equal contributors.

Received October 10, 2024; Accepted November 25, 2024; Epub December 15, 2024; Published December 30, 2024

Abstract: Prostate cancer (PCa) is the second leading cause of cancer-related deaths among American men. The development of metastatic castration resistant PCa (mCRPC) is the current clinical challenge. Antiandrogens such as Enzalutamide (ENZ) are commonly used for CRPC treatment. However, patients with androgen receptor (AR)-negative tumors do not respond to ENZ, while AR-positive tumors frequently develop resistance, limiting the long-term efficacy of this therapy. This study investigates the efficacy of neutral sphingomyelinase 2 (n-SMase2) inhibition by DPTIP, both alone and in combination with ENZ, as a therapeutic strategy for mCRPC. *In vitro* assays were conducted to determine the half-maximal inhibitory concentration (IC_{50}) of DPTIP and ENZ in mCRPC cells. The effect of these treatments on cell proliferation, migration, and colony formation was assessed. The antitumor effect of DPTIP was also evaluated in a preclinical PCa mouse model. Elevated n-SMase2 expression was observed in PCa patients compared to normal subjects at both mRNA and protein levels. In CWR-R1ca and PC-3 cells, DPTIP had IC_{50} values of 10.31 and 14.57 μM, while ENZ had IC_{50} values of 33.7 and 81 μM, respectively. Combined treatment significantly suppressed cell proliferation, colony formation, and migration of mCRPC cells. Mechanistically, the ERK1/2 activity and the expression of nSMase2 and NF-kB p65 were inhibited by DPTIP. The *in vivo* combination of DPTIP and ENZ reduced tumor size and weight more effectively than either drug alone, without significant changes in body weight. This study highlights the therapeutic potential of targeting n-SMase2 for mCRPC. Inhibition of n-SMase2 using DPTIP, both as a standalone treatment and in combination with ENZ, effectively suppressed the growth and migration of mCRPC cells. These findings suggest a promising novel approach to treating mCRPC and warrant further investigation in clinical settings.

Keywords: Prostate cancer, mCRPC, n-SMase2, DPTIP, Enzalutamide, mouse model

Introduction

Prostate cancer (PCa) is one of the leading causes of cancer-associated deaths in American men [1]. Androgen signaling, mediated *via* androgen receptor (AR), is the main driving force for PCa progression and metastasis [2]. Systemic therapies have been used as an option for PCa management. However, chemotherapy is the ultimate solution, especially in patients with castration resistant PCa (CRPC) [3]. Although the circulating androgen level is extremely low in these patients, it is still sufficient for inducing AR signaling and maintaining tumor cell growth. The first-line therapeutic option for treating CRPC patients is anti-androgen therapy, including Enzalutamide (ENZ, MDV3100; Xtandi®). However, clinical responses to ENZ vary significantly. Up to 25% of patients develop *de novo* resistance against

https://doi.org/10.62347/XXXA3182

ENZ, and other patients who initially responded are more likely to develop acquired resistance within months of treatment [4]. The development of metastatic CRPC (mCRPC) warrants the discovery of new therapies for treating mCRPC patients.

Sphingomyelinases catalyze the hydrolysis of sphingomyelin to ceramide and phosphorylcholine. Neutral sphingomyelinase 2 (n-SMase2), a subfamily of sphingomyelinase, is associated with cellular stress response, ceramide-mediated apoptosis, inflammation, neurological disorders, sEV biogenesis, cancer development, and metastasis [5-8]. Recent n-SMase2 inhibitor, 2,6-dimethoxy-4-(5-phenyl-4-thiophen-2-yl-1H-imidazole-2-yl)-phenol (DPTIP) inhibits the biogenesis of small extracellular vesicles in different pathophysiological conditions [9].

The drug combination is a highly effective approach to tackle the heterogeneity of prostate cancer and reduce drug resistance development. For example, ENZ was combined with different agents to target aggressive cancer cells [10, 11]. Using a drug repurposing strategy, a combination of vasodilator hydralazine with ENZ showed a synergistic effect on PCa cells [11]. In another study, combining HIF-α inhibitor NLG207 with ENZ was more effective in pre-clinical PCa mouse models of ENZ resistance [12]. A novel nonpharmaceutical of camptothecin (CRLX101) combined with ENZ was also used in a clinical trial to treat CRPC patients (NCT03531827). In 2023, the FDA approved the combination of ENZ and PARP inhibitor talazoparib for mCRPC patients with homologous recombination repair (HRR) gene mutations (NCT03395197) [13]. Hence, novel therapies are urgently needed to target dysregulated molecular pathways in aggressive PCa cells and to reduce drug resistance.

In this study, we explored the potential of DPTIP as monotherapy and in combination with ENZ to target n-SMase2-mediated pathways in mCRPC. We investigated the expression of n-SMase2 in human tissues of PCa and normal adjacent tissues on mRNA and protein levels. The results show that n-SMase2 was overexpressed in PCa compared to normal tissues. *In vitro* studies revealed that the combination of DPTIP and ENZ was effective at 0.1 IC_{50} and reached the maximum at 0.5 IC_{50} value. When the two drugs were combined, significant n-SMase2, NF-kB, and ERk1/2 inhibitions were observed. RNA-seq analysis showed dysregulated RNA and pathways affected by DPTIP treatment compared to vehicle control cells. In a preclinical PCa model, treating mice with DPTIP reduced the tumor size and weight but did not affect the total body weight.

Materials and methods

Reagents

Cell culture media, antibiotics, and fetal bovine serum (FBS) were obtained from authenticated commercial sources. Enzalutamide (Cat#HY-70002) and 2,6-Dimethoxy-4-(5-Phenyl-4-Thiophen-2-yl-1H-Imidazol-2-yl)-Phenol (DPTIP, Cat# HY-131002) were purchased from MedChemExpress (Monmouth Junction, NJ, USA). MTT 3-(4,5-Dimethylthiazol-2-yl)-2,5-Diphenyltetrazolium Bromide (Cat#M6494) was purchased from ThermoFisher Scientific (Waltham, MA, USA).

Evaluating SMPD3 gene expression in PCa tissues

The expression of *SMPD3* transcript in human PCa tissues was evaluated by retrieving data available from the online UALCAN based on the TCGA database (https://ualcan.path.uab.edu/) according to Chandrasekhar *et al.* [14, 15]. The transcript per million (TPM) enrichment analysis was used for reporting gene expression according to the sample type, Gleason score (GS), nodal metastasis status and molecular signature.

Cell culture

PCa cell lines PC-3M, PC-3, and CWR-22RV1, in addition to RWPE1 normal cells, were obtained from the American Type Culture Collection (ATCC). CWR-R1ca was purchased from Millipore Sigma (Burlington, MA, USA). RWPE1 cells were grown in a keratinocyte serum-free medium containing 50 µg/mL bovine pituitary extract and 5 ng/mL human epidermal growth factor. The normal prostate epithelial PNT1A cells were maintained in RPMI-1640 medium with 2 mM L-glutamine as described [16]. PCa cells were grown in DMEM medium supplemented with 10% FBS and antibiotics and maintained in a humidified incubator at 37°C with a 5% CO_2 supply.

Cell proliferation assay

Cytotoxicity assay was performed to measure the effect of the drugs on cell proliferation in the control and treated cells. The cells were seeded in a 96-well plate and treated with different concentrations of DPTIP and ENZ for three days. 3-(4,5-Dimethylthiazol-2-yl)-2,5-Diphenyltetrazolium Bromide (ThermoFisher Scientific) was added into each well, after which the formazan crystals were solubilized, and the optical density was measured, using a spectrophotometric plate reader (AccuSkan FC plate reader, ThermoFisher Scientific, Waltham, MA) at 450 nm. The half-maximal inhibitory concentration (IC_{50}) values for each drug were calculated using GraphPad Software. The difference between the control and treated cells was expressed as a percentage of change.

Colony-formation assay

To assess the effect of ENZ and DPTIP on colony formation, CWR-R1Ca, CWR-22RV1, PC-3, and PC-3M were seeded in 6-well plates (500 cells/well). After 2 days, they were treated with ENZ and DPTIP at various concentrations and kept in a cell incubator for another two weeks. The cells were fixed with 4% paraformaldehyde for 10 minutes and then stained with 0.5% crystal violet for 20 minutes. The stained colonies were rinsed with tap water and left overnight to dry out. The number of colonies was then calculated using ImageJ software (US National Institutes of Health).

Cell migration assay

The Boyden chamber assay was performed to assess the effect of DPTIP and ENZ on cell migration of mCRPC cells according to our prior study [17]. Briefly, about 1.0×10^5 cells were suspended in serum-free medium provided with filtered 0.1% BSA and seeded in the upper transwell chamber for 24 h with 0.5 IC_{50} of DPTIP or ENZ, while the lower one contained complete 10% FBS medium. The migratory cells on the bottom of each insert were fixed in 4% paraformaldehyde solution, stained with 0.5% crystal violet, washed twice with water, and kept at room temperature to dry. The migrated cells were counted and photographed. The wound-healing assay was performed on mCRPC cells in another set of experiments. The cells were grown in 6-well plates until they reached 80-90% confluency, after which a pipette tip was used to create a scratch wound on the cell monolayer. Images of the wound were captured at various time points (0-48 hours) and the relative width of the wound was measured by ImageJ Software. The changes in wound width (μm) were calculated by dividing the average wound width at each time point by the initial wound width.

Immunoblot analysis

After the treatment of cells with DPTIP and ENZ, alone or in combination, for 24 and 48 hours, the cells were rinsed with PBS and lysed. Protein expression was analyzed by separating 30 μg protein lysates using SDS-PAGE and transferring the resolved proteins onto PVDF membranes. Non-specific binding was blocked with 5% BSA, and the blots were then incubated overnight with anti-n-SMase2 primary antibodies (Cat#orb158038) purchased from Biorbyt (Durham, NC, USA). Anti-NF-kB (Cat#3034), anti-ERK1/2 (Cat#4696), anti-phosphorylated ERK1/2 Thr202/Tyr204 (Cat#4376), anti-AR (Cat#5153), and anti-AR-V7 (Cat#19672) antibodies were purchased from Cell signaling Technology (Danvers, MA, USA). The blots were then washed and incubated with the appropriate secondary antibodies for 1 hour at room temperature. The protein signal was developed using a Clarity ECL Western Blotting substrate kit and visualized by Bio-Rad ChemiDoc imager (Bio-Rad, Hercules, CA, USA).

Immunohistochemistry (IHC)

The human tissue microarray (TMA) slide comprising 100 cases of PCa tissue cores, 7 BPH, and 11 standard and tumor-adjacent tissue cores were purchased from commercially available sources (US Biomax, Inc., Derwood, MD). The clinical characteristics of PCa patients are provided in Table S1. The IHC technique was performed according to our previous study [18]. In brief, tissue sections were de-waxed in two cycles of xylene and rehydrated in a descending series of ethanol solutions. The TMA slide was then heated in ethylenediaminetetraacetic acid (EDTA) buffer (pH 8.0) for 25 minutes. The slide was incubated in 3% peroxide for blocking tissue endogenous peroxidase activity. After thoroughly washing and serum blocking, the slide was incubated overnight at 4°C with n-SMase2 primary antibody (Santa Cruz

Biotechnology). The developed antigen-antibody complex was detected by a commercially available Vectastain Elite ABC HRP kit (Vector Laboratories, Burlingame, CA, USA). The slide was then counterstained with hematoxylin and mounted in a permanent mounting medium. The developed protein signals were acquired using an AmScope microscope with a camera (AmScope, Irvine, CA). The stained tissues were blindly examined, and the histochemical score (HSC) was calculated as reported [19].

RNA-Seq analysis

To identify unique coding and non-coding RNAs associated with n-SMase suppression, total RNA was extracted from PC-3M cells treated with 0.1 IC_{50} DPTIP in addition to vehicle control cells for 24 hours. For each sample, 1 µL of the final RNA eluate was used to measure mRNA concentration by Agilent Bioanalyzer 2100 (Agilent Technologies, Santa Clara, CA). RNA libraries were constructed with the CleanTag Small RNA Library Preparation Kit (TriLink, San Diego, CA) according to the manufacturer's protocol. The final purified library was quantified with High Sensitivity DNA Reagents and High Sensitivity DNA Chips (Agilent Technologies). The libraries were pooled, and the 140 to 300 bp region was size selected on 8% TBE gel (Invitrogen). The TailorMix HT1 qPCR assay (SeqMatic, Fremont, CA) was used, followed by a NextSeq High Output single-end sequencing run at SR75 using NextSeq 500/550 High Output v2 kit according to the standard protocol (Illumina, San Diego, CA). Sequencing data was uploaded into the UCSC analysis pipeline and analyzed [20]. RNA-seq analysis was performed at the Tulane University Aging Center, New Orleans, LA, USA. For a given comparison, a positive fold change value indicates an increase in expression, while a negative fold change indicates a decrease in expression. Pathway analysis was performed using Gene Set Enrichment Analysis (GSEA) and Gene Ontology (GO).

RNA isolation and gene expression

Total RNA from PCa cells was extracted using TRIzol Reagent (Invitrogen, Cat. #15596026) according to the manufacturer's protocol. RNA was quantified on a NanoDrop spectrophotometer (Thermo Fisher Scientific). cDNA was synthesized using oligo(dT) and random primers approach using iScript Reverse Transcription Supermix (Cat. #170884, Bio-Rad, Hercules, CA) PrimerQuest tool from Integrated DNA Technologies was utilized to design primers for the gene expression, with the GAPDH gene serving as an internal reference. The sequences of primers used int his study are presented in Table S2. Quantitative Real-Time polymerase reaction was performed using 2× SYBR Green qPCR Master Mix (Cat. #B21202, Selleck, Houston, TX) under the following conditions: denaturation: 95°C for 2 min, followed by 40 cycles of denaturation at 95°C for 15 s and annealing at 60°C for 30 s using qPCR (QuantStudio 3, Applied Biosystems, Waltham, MA). Relative gene expression was determined using the ΔΔCT method. The change in gene expression was calculated as a relative fold difference regarding housekeeping *gapdh* gene.

Establishment of cell-expressing luciferase

Stable luciferase-bearing CWR-R1Ca cells were established as described [21]. Lentiviral particles carrying luciferase from Kerafast (Boston, MA, USA) were briefly transduced into PCa cells, followed by puromycin selection. Cells with luciferase bioluminescence were examined using the Perkin Elmer InVivo machine (IVIS; PerkinElmer, Waltham, MA).

Preclinical study

Animal experiments were carried out using an IACUC protocol approved by the Institutional Animal Care and Use Committee of the University of Louisiana at Monroe (IACUC approval #21AUG-ZE-01). About 4-6-week-old male nude mice were purchased from Envigo (Indianapolis, IN, USA). About 50 µL of CWR-R1ca-luciferase cells (2×10^6 cells) mixed with an equivalent volume of Matrigel™ (BD Bioscience) kept on ice were injected into the dorsal flank of each mouse. The individual and combined drugs were intraperitoneally administered daily for 3 weeks. Animals were divided into 4 groups: 5 mice each. Group 1 received a vehicle; Group 2 received 10 mg/Kg ENZ, as reported [22, 23]; Group 3 received 10 mg/Kg DPTIP according to a previous study [9]; and Group 4 received 10 mg/Kg ENZ combined with 10 mg/Kg DPTIP. After 1 and 3 weeks from initiating the treatment, D-luciferin (10 µL/g body weight) was intraperitoneally injected, and after 10 minutes, bioluminescent

images were acquired using an In Vivo Imaging System (IVIS; PerkinElmer, Waltham, MA). During the experiment, mice were weighed, and tumor volume was calculated twice a week using the formula π/6 ($L \times W^2$) as described [24]. The tumor mass was collected, and one piece was fixed in 10% neutral formalin for histopathological studies, while the other pieces were snap-frozen for biochemical analyses.

Statistical analysis

Data presented as mean ± standard error of the mean (SEM). Statistical comparisons between experimental and control groups were performed using an unpaired Student's *t*-test. For multiple group comparisons, one-way analysis of variance (ANOVA) was used, followed by Tukey's post-hoc test to correct for multiple comparisons. Statistical significance was determined at $P<0.05$. All statistical analyses were conducted using GraphPad Prism version 10.10.0 for Windows (GraphPad Software, Boston, Massachusetts, USA).

Results

Expression of n-SMase2 in human PCa tissues

We investigated the expression n-SMase2, encoded by SMPD3 gene, in available human cancers (Figure S1) and in PCa tissues and normal adjacent cores on both the mRNA and protein levels using TCGA available data and human tissue microarray (TMA). SMPD3 transcript was upregulated in pancreatic cancer, PCa, pheochromocytoma and sarcoma compared to normal tissues. TCGA data analysis showed that SMPD3 was upregulated in PCa ($P<0.0001$) compared to normal tissues (**Figure 1A**). Notably, SMPD3 expression was elevated across different tumor stages using Gleason score (GS) 6 to 9 ($P=0.019$) when compared to normal individuals. However, we found no statistically significant differences in lymph node involvement based on SMPD3 expression levels in the analyzed tissues. Regarding molecular signatures, SMPD3 was found to be upregulated in tissues associated with ETS-related gene (ERG) fusions, PEA3 subfamily ETV1 & 4, and Friend Leukemia Integration 1 (FLI1) gene fusions. On the protein level, the immunostaining of TMA tissue cores with an n-SMase2 antibody revealed high expression in tissues collected from patients with GS 7, moderate expression in GS 9 tissues, and low expression in normal and benign hyperplastic prostate tissues (**Figure 1B**). Immunohistochemical score (IHS) was used to evaluate the protein expression in PCa tissues as reported [19, 25]. The IHS of n-SMase2 was high in PCa, confirming the mRNA level results. Despite the findings indicating varying levels of n-SMase2 expression, there was no significant difference in protein expression based on age at diagnosis, Gleason score, lymph node involvement, or metastatic status (**Figure 1C**). This suggests that n-SMase2 may play a role in the pathogenesis of PCa at early stages, independent of these clinical factors. These observations support the notion of targeting n-SMase2 as an evidence-based therapeutic approach, potentially providing a strategy for intervention in the early progression of the disease.

Effect of DPTIP combination with ENZ on mCRPC cells

To establish effective dosing parameters for DPTIP and ENZ, we first determined the IC_{50} values for the two drugs across multiple mCRPC cell lines, including PC-3, PC-3M, CWR-22RV1, and CWR-R1Ca, as well as normal prostate epithelial (PNT1A) cells. Cells were treated with different concentrations of DPTIP or ENZ at a concentration range from 0-250 μM for up to 72 hours, and IC_{50} values were calculated based on cell viability assay [18] as shown in **Table 1**. The IC_{50} values for PC-3 and its highly metastatic derived PC-3M cells recorded the highest values compared to CWR-22RV1 and CWR-R1ca cells (IC_{50} value range from 31 to 34 μM) because they lack AR as a constitutive target. The IC_{50} value of ENZ was the highest in normal prostate PNT1A cells, which indicates the drug's selectivity towards tumor cells. The same pattern was observed in PNT1A treated with DPTIP (IC_{50}=27.1 μM) compared to PCa cells. Based on these results, concentrations corresponding to 0.1 and 0.5 IC_{50} were selected for subsequent experiments. To assess the potential synergistic effects of DPTIP and ENZ, mCRPC cells were treated with drug individually at 0.1 and 0.5 IC_{50} as well as in combination. As shown in **Figure 2**, the most practical combination of the two drugs was observed in CWR-22RV1 (**Figure 2A**) and CWR-R1Ca (**Figure 2B**) cells at the concentration of 0.5 IC_{50} of either drug ($P<0.001$) when compared to

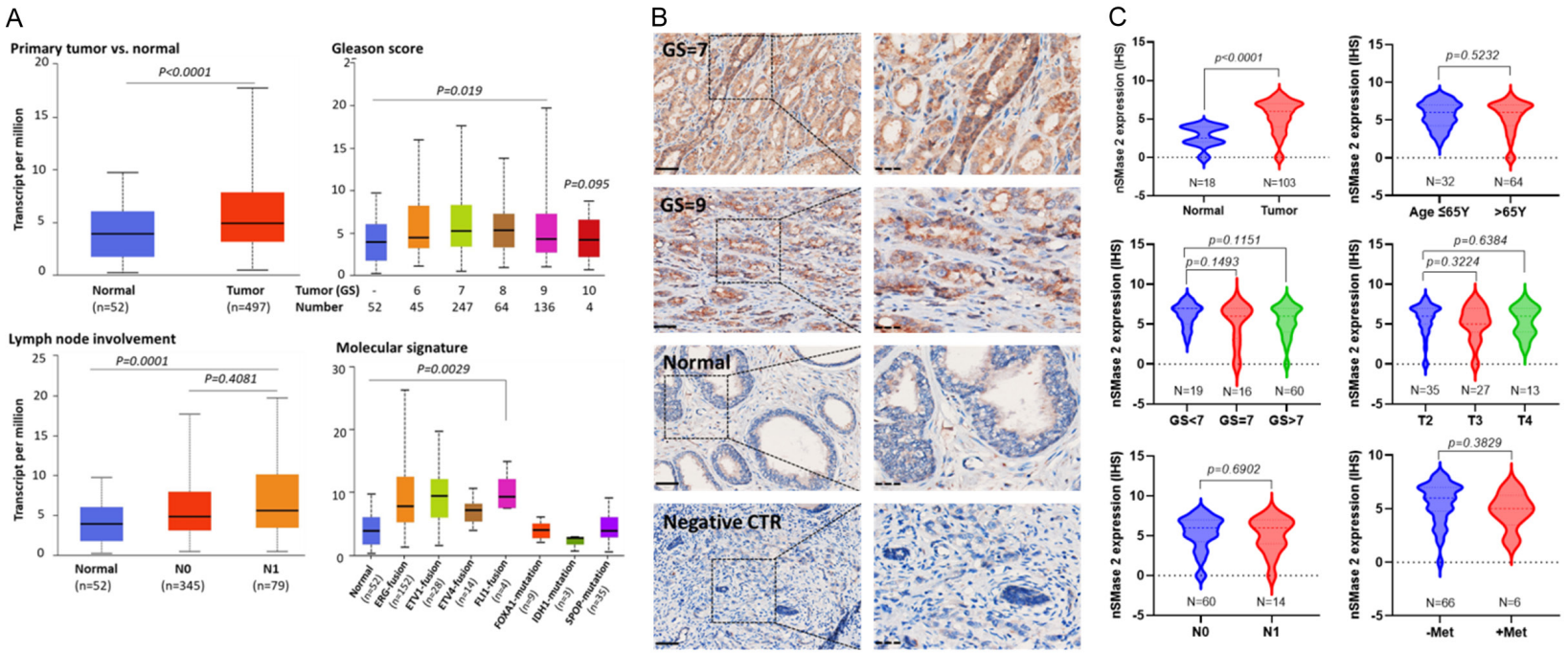

Figure 1. Expression of n-SMase2 in human PCa tissues. A: Expression of n-SMase2 gene SMPD3 transcript retrieved from TCGA data of PCa compared to normal tissues. B: The protein expression of nSMase2 was evaluated by immunohistochemistry in tissue microarray slide comprising 100 cases of PCa tissue cores, 7 BPH, and 11 normal and tumor adjacent tissues cores. The protein expression was represented according to Gleason score (GS). Another slide was incubated only with secondary antibody and kept as a negative control (CTR). C: The immunostaining of nSMase2 was expressed as immunohistochemical score (IHS) which was used to compare PCa with normal tissues, age at diagnosis, Gleason score (GS), pathological stages (T2-4), lymph node metastatic status and distant metastasis (Met). Quantification of immunohistochemical score of n-SMase2 staining. Magnification is 50 μm (solid line) and 20 μm (dashed line). Data considered significant at P<0.01 regarding control groups. N: number; N0/N1: involvement of lymph nodes.

Table 1. Determination of IC_{50} for DPTIP and enzalutamide in mCRPC cells

Cell line/IC_{50}	DPTIP (μM)	Enzalutamide (μM)
CWR-22RV1	9.80	31.8
CWR-R1ca	10.31	33.7
PC-3	14.57	81
PC-3M	15.27	95
PNT1A	27.14	220

individual treatments. To understand the differential response to DPTIP treatment, Western blotting analysis examined the expression of n-SMase2 in different PCa and normal cells. The protein expression was markedly low in RWPE1 normal cells, moderate in CWR-22RV1 and CWR-R1Ca cells, and high in PC-3 and PC-3M cells (**Figure 2C**, **2D**). The expression of AR and its variant AR-V7 was also validated in these cells by immunoblot analysis.

Effect of DPTIP and ENZ on colony formation and cell migration

To assess the long-term anti-proliferative effects of DPTIP and ENZ, colony formation assay was performed. AR-expressing CWR-22RV1 cells were treated with 0.1 and 0.5 IC_{50} of DPTIP and ENZ, either alone or in combination, and allow to grow for up to 14 days. As shown in **Figure 3**, the treatment of cells with individual drugs decreased the number and size of colonies, and this effect increased at 0.5 IC_{50} value of each drug. Interestingly, the drug combination at 0.5 IC_{50} value showed a 90% decrease in the number and size of colonies compared to individual drug treatments. The same effect was observed in AR-naïve PC-3 cells, where the drug combination at 0.5 IC_{50} value showed a 96% colony number reduction. Regarding cell migration, a Boyden chamber assay was performed on CWR-R1Ca and PC-3 cells (**Figure 4**). The individual treatment of cells with 0.5 IC_{50} values of ENZ or DPTIP decreased migratory cells by 50 and 68%, respectively. Cells treated with the combined drugs showed an 85% reduction in cell migration compared to single treatment. Another confirmatory experiment was conducted on PC-3 cells using a scratch assay. Cells were seeded in a 6-well plate, and once they reached confluency, a scratch assay was performed. Cells treated with individual or combined drugs and photographed after 0, 24, and 48 h of treatment. Treating cells for 48 h with 0.5 IC_{50} of the combined drugs reduced cell motility by 35% and 72% compared to single treatment and vehicle control cells, respectively (Figure S2).

Effect of DPTIP on ERK1/2 activity and NF-kB expression

To confirm the inhibitory effect of DPTIP on the protein expression of n-SMase2, immunoblotting analysis was performed on PC-3M cells which have a relative high endogenous n-SMase2 level (**Figure 5**) compared to low n-SMase2 level in CWR-R1Ca cells (Figure S3). Treatement of PC-3M cells with DPTIP for 24 and 48 h exhibited a significant inhibition in n-SMase2 expression when treated with DPTIP compared to ENZ-treated cells. This effect was augmented after the two drugs were combined at 0.1 or 0.5 IC_{50} (**Figure 5**). Since MEK-ERK and NF-kB singlaing pathway contribute to deveopment and progression of mCRPC and reported as therapetuc targets [26], we selected to assess the inhbitory effect of DPTIP on these pathways. While the activity of ERK1/2 showed a relative inhbition in cells treated with either drug individually, the ERK1/2 activity was markedly decreased when the two drugs were combined. This effect was increased after 48 h of drug tretament. NF-kB expression was reduced after DPTIP but not ENZ treatment and the drug combination showed a further reduction at 0.5 IC_{50} of both drugs. Treatment of CWR-R1Ca cells for 24 h had different pattern of protein expression comapred to PC-3M as shown in Figure S3. The expression of n-SMase2 was decreased 0.5 IC_{50} of the combined drugs while NF-kB expression was reduced when cells treated with 0.5 IC_{50} of DPTIP and reached the maxium with 0.5 IC_{50} of ENZ treatment.

The treatment of mCRPC cells with DPTIP induces gene dysregulation and targets multiple signaling pathways

The treatment of PC-3M cells with 0.1 IC_{50} DPTIP for 24 h changes the expression of coding and non-coding RNAs. The most upregulated and downregulated genes are listed in Table S3 and illustrated in **Figure 6**. Among the most upregulated genes as shown in **Table 2**, exonuclease 5 (Exo5) which showed a 14-fold increase in DPTIP-treated cells. The function of

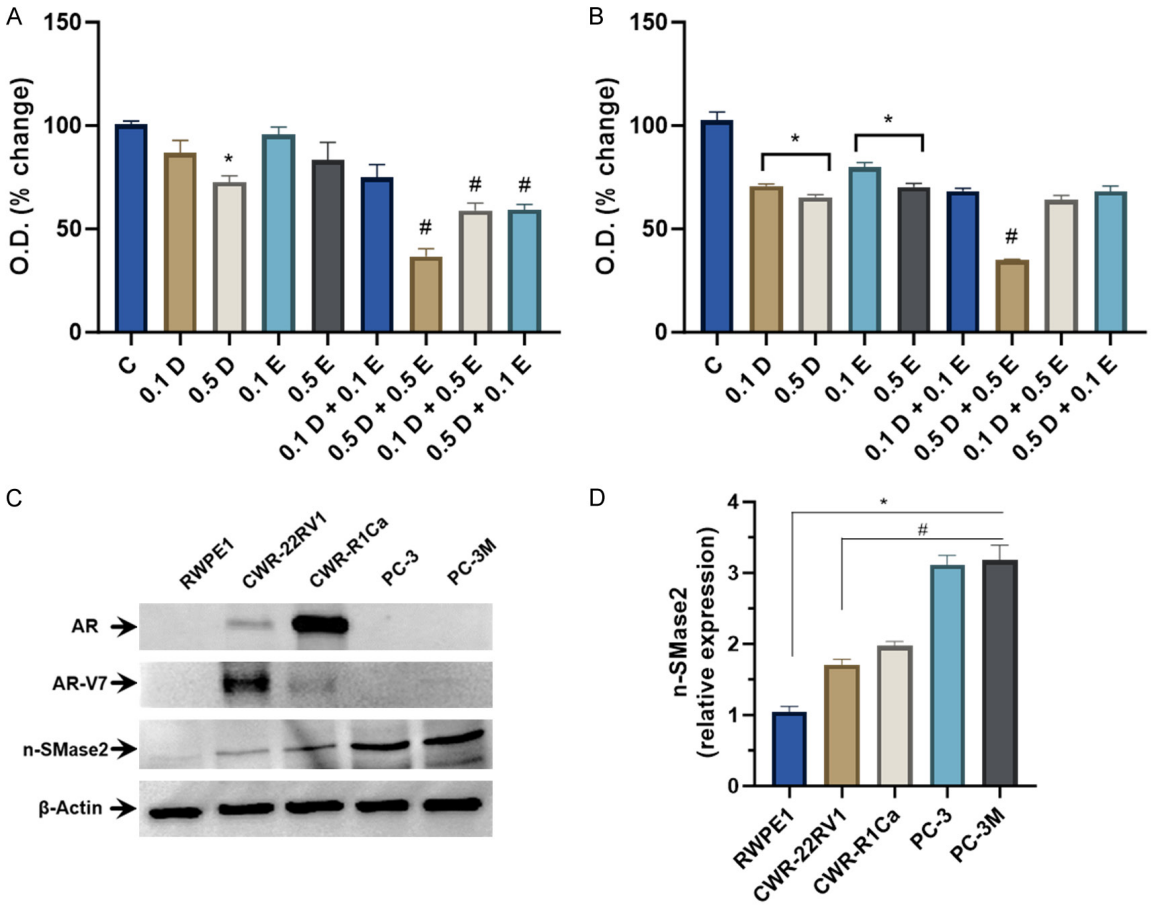

Figure 2. Cytotoxic effect of treatment of mCRPC cells with combined drugs. (A, B) CWR-22RV1 (A) and CWR-R1Ca (B) cells were treated with 0.1 and 0.5 of IC_{50} of DPTIP (D) or enzalutamide (E), individually and in combination, for 72 hours. Cell viability assay was performed as indicated and the percentage of O.D. change relative to control cells was calculated. (C) Western blot analysis was performed for AR, AR-V7 and n-SMase2 expressions. β-actin was used as loading control. (D) The endogenous expression of n-SMase2 was calculated relative to the house keeping protein and expressed as arbitrary unit compared to the control cells. *, # denote significance at $P<0.05$ relative to vehicle control cells and individual treatment, respectively.

Exo5 is to assist in repairing nuclear DNA damage caused by external stimuli [27]. Additionally, fibulin 7 (FBL7) and killer cell lectin-like receptor C1 (KLRC1) were both upregulated by 10-fold. Conversely, coding mRNA Nox organizer 1 (NOXO1) and non-coding long intergenic non-protein coding RNA 482 (LINC00482) were significantly downregulated. Previous studies have shown that the Nox1 inhibitor NOS31 selectively inhibits Nox1-mediated reactive oxygen species (ROS) generation, which is closely associated to NOXO1 function in colon cancer cells [28]. Moreover, a group of researchers identified a set of upregulated non-coding RNAs, including LINC00482, which was associated with biochemical relapses in PCa patients [29]. **Figure 6A** and **6B** shows the identified molecular pathways and their associated genes in cells treated with DPTIP. These pathways include E2F, G2M, MYC, and estrogen response pathways. To further validate these findings, we evaluated the expression of the most relevant genes associated with PC-3M-treated cells with DPTIP, ENZ and their combinations (**Figure 6C**). qPCR analysis revealed that FBLN7, KLRC, C10orf90 and TBX4 genes were upregulated while NOXO1 was downregulated after DPTIP treatment for 48 h compared to vehicle control cells.

Effect of DPTIP and ENZ on tumor size in nude mice

To validate the *in vitro* findings, we conducted in vivo experiments using a nude mouse xenograft model. Male nude mice were injected sub-

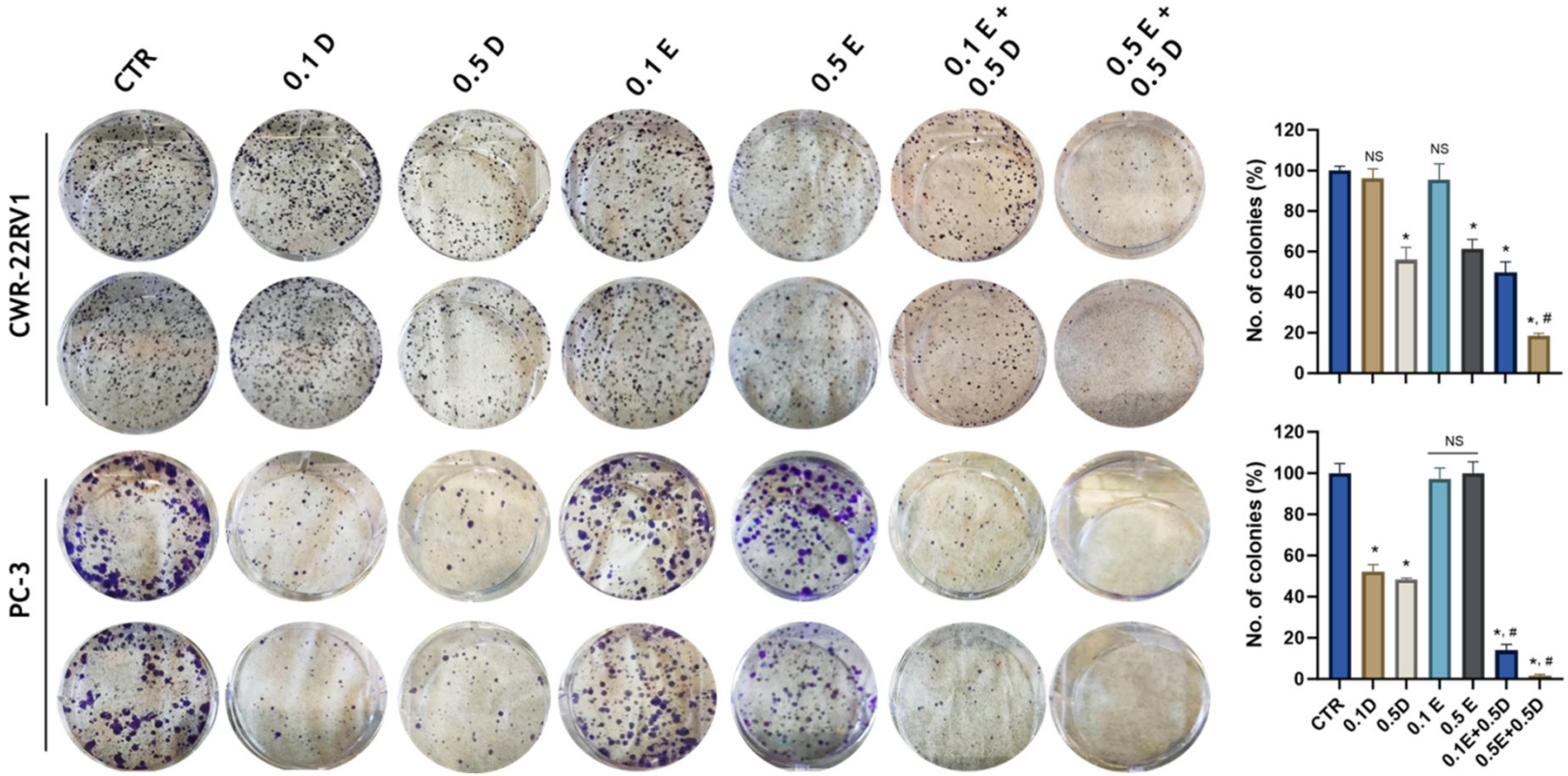

Figure 3. Effect of treatment of mCRPC cells with DPTIP and Enzalutamide on colony formation. CWR-22RV1 and PC-3 cells were treated with 0.1 and 0.5 IC_{50} of DPTIP (D) and Enzalutamide (E), and their combinations for 14 days, fixed, stained and dried out for imaging. The number and size of cell colonies were counted and presented as mean + SEM as indicated in bar graphs. *, # depict statistical significance at $P<0.05$ regarding vehicle control or individual treatment, respectively. Each treatment was conducted in duplicate, and the experiment was independently repeated twice.

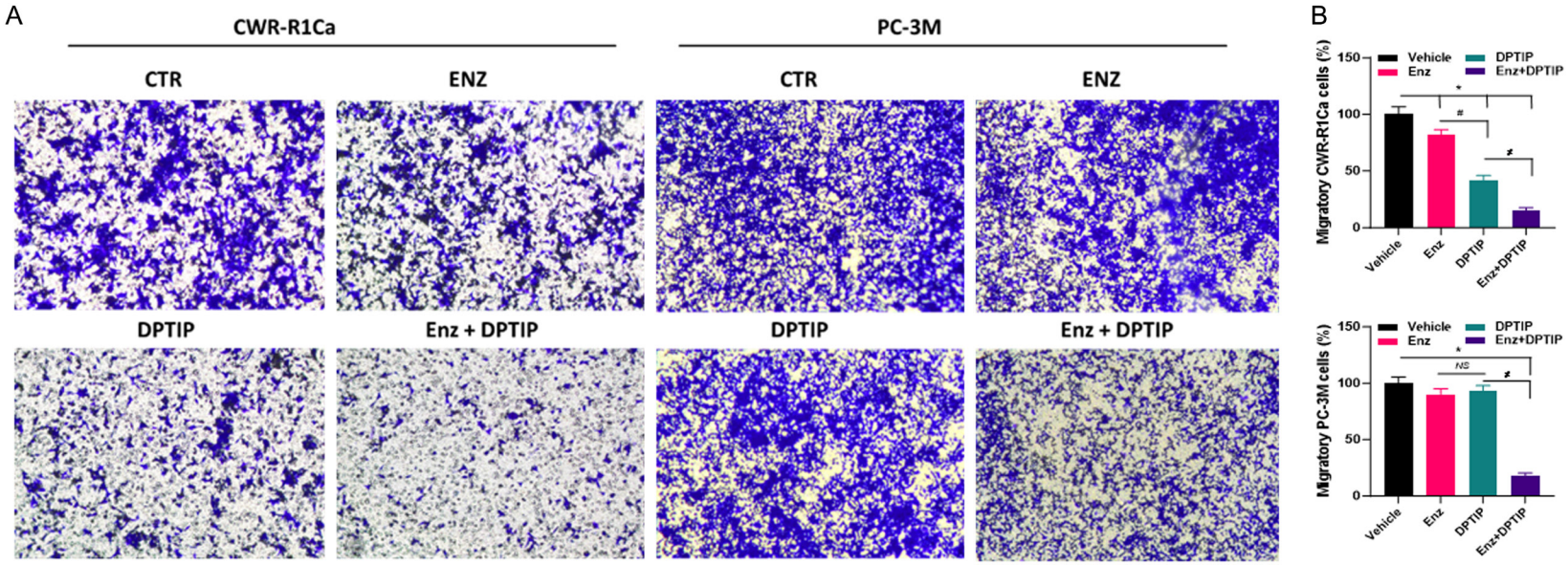

Figure 4. Effect of DPTIP and ENZ on mCRPC cell migration. A: About 5 × 10^4 cells were seeded in upper insert in FBS-depleted medium while complete medium was added to lower wells. Cells were treated with 0.5 IC_{50} of DPTIP and ENZ, and their combinations for 36 h. The migrated cells were fixed, stained, and imaged. B: The migrated cells were counted and presented as percentage of migratory cells. *, #, ≠ depict significance at $P<0.05$ compared to vehicle control, ENZ and DPTIP, respectively. NS: Nonsignificant. Magnification was 100×.

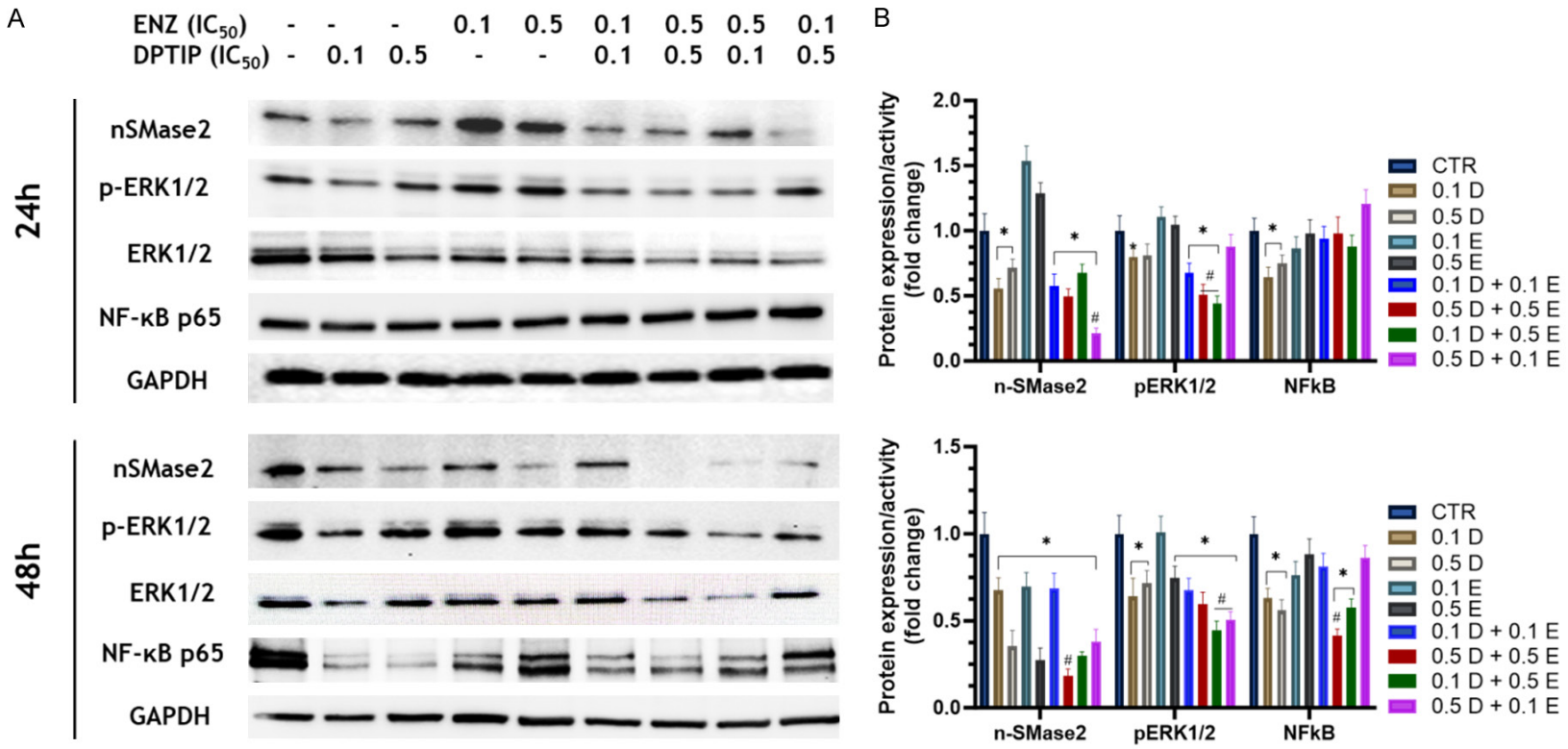

Figure 5. Molecular effect of DPTIP and Enzalutamide treatments on PC-3M cells. A: Cells were treated with 0.1 and 0.5 IC_{50} of DPTIP (D) and Enzalutamide (E), and their combinations for 24 and 48 h. Cell lysates were collected and subjected to Western blot analysis. The membrane-bound proteins were incubated with antibodies against nSMase2, phosphorylated and total ERK1/2, and NF-kB p65. B: The relative expression was calculated as fold change relative to control cells and represented as mean ± SEM as indicated in bar graphs. *, # depict statistical significance at $P<0.05$ regarding vehicle control or individual treatments, respectively.

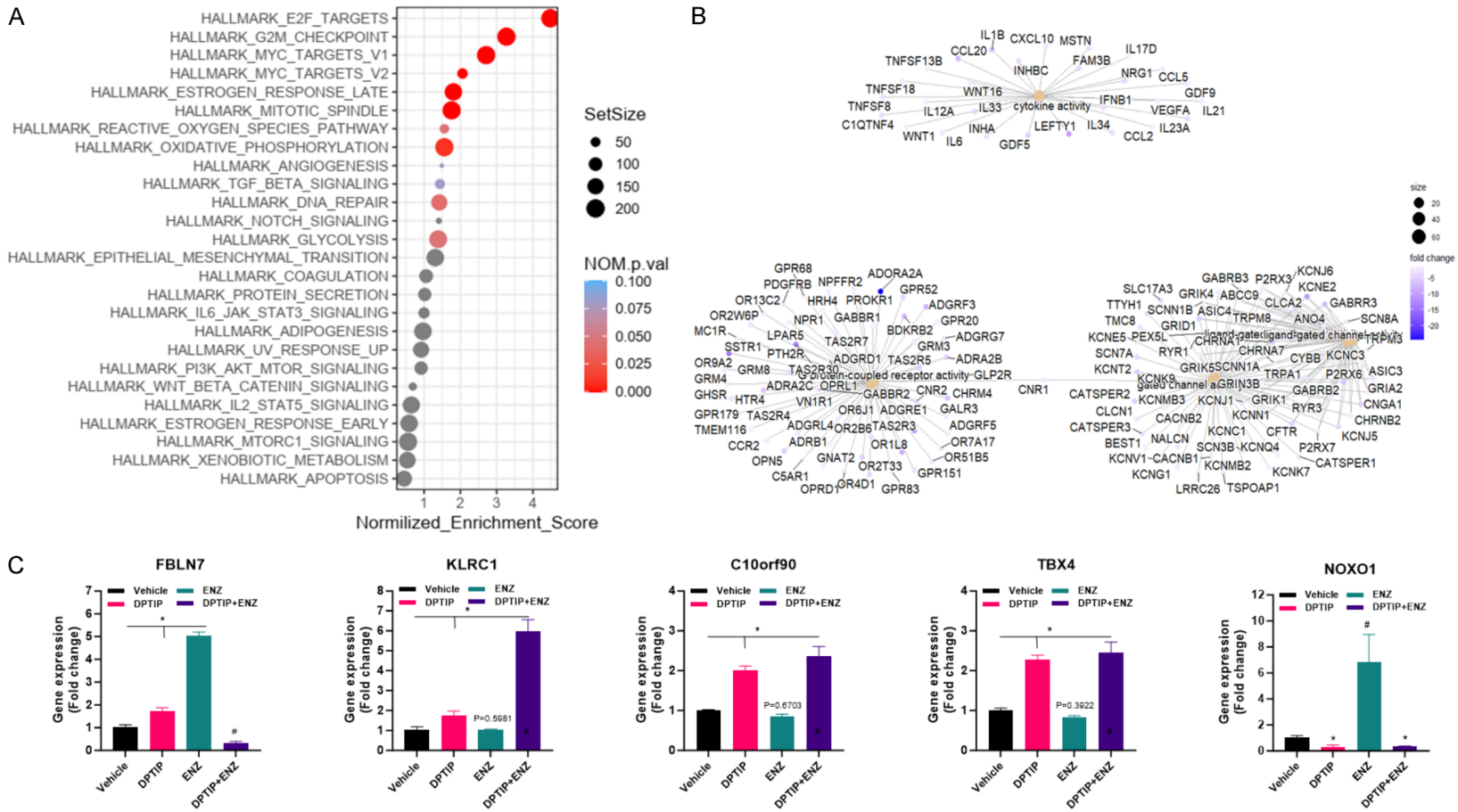

Figure 6. RNA-seq and molecular pathways in mCRPC cells treated with DPTIP. A: Visualizing GSEA enrichment results for DPTIP-treated vs. vehicle control PC-3M cells using ggplot2. B: Top five non-redundant enriched terms for the GO class molecular function. C: Quantitative Real-Time PCR analysis was performed as indicated and presented as fold change to cells received vehicle. *, # depict significance at P<0.01 regarding vehicle control cells.

Table 2. Top listed up- and down-regulated RNAs after treatment of PC-3M cells with DPTIP

	Gene	Description	Log FC	RNA
1	Exo5	Exonuclease 5	+14	Coding
2	FBLN7	Fibulin-7	+10	Coding
3	KLRC1	Killer Cell Lectin Like Receptor C1 (NKG2A)	+10	Coding
4	C10orf90	The fragile-site associated tumor suppressor	+9	Coding
5	TBX4	T-Box Transcription Factor 4	+8	Coding
6	HTR2C	5-Hydroxytryptamine Receptor 2C	+5	Coding
7	NOXO1	Nox organizer 1	-5	Coding
8	LINC00482	Long Intergenic Non-Protein Coding RNA 482	-7	Non-coding
9	GIMAP2	GTPase, IMAP Family Member 2	-8	Coding
10	DPT	Dermatopontin	-8	Coding

RNA-seq analysis of PC-3M cells treated with DPTIP compared with untreated cells.

cutaneously with CWR-R1Ca cells. Once the tumor size became palpable, the mice were treated with intraperitoneal injections of DPTIP and ENZ at a dose of 10 mg/kg/mouse, either individually or in combination, for 3 weeks (**Figure 7A**). Prior to sacrifice, D-luciferin was intraperitoneally injected, and live images were acquired (**Figure 7B**). Mice treated with single DPTIP or ENZ, revealed significant tumor size reductions of 29.6 and 34.3%, respectively, compared to vehicle-treated control (**Figure 7C**). The combination of DPTIP and ENZ further reduced tumor size by 45.3%. Notably, the two drugs did not elicit any significant changes in body weight, which implies the safety levels of the injected doses of single and combined drugs (**Figure 7D**). After the mice were sacrificed, tumors were resected and weighed. DPTIP and ENZ showed a significant reduction in tumor weight, and although their combination further decreased the tumor weight, it did not reach statistical significance when compared to either drug alone (**Figure 7E**).

Discussion

Our findings highlight the significant role of n-SMase2 and its encoded gene SMPD3 in PCa, particularly its overexpression in PCa, especially at GS 7, in comparison to other tissues. The combination of the nSMase-2 inhibitor DPTIP with enzalutamide (ENZ) shows promise, with optimal efficacy observed at 0.5 IC_{50} for both drugs. The data demonstrate that treatment with either DPTIP or ENZ effectively inhibits cell proliferation and migration in mCRPC cells, with even greater effects observed with the combination treatment. Furthermore, the *in vivo* studies with CWR-R1Ca xenografts support the notion that DPTIP contributes to tumor size reduction, indicating its potential as a therapeutic agent in PCa treatment.

High ceramide levels are associated with aggressive PCa forms, failure in lowering testosterone levels in metastatic hormone-sensitive PCa, and shorter survival time in mCRPC [30]. Sphingomyelinases catalyze the hydrolysis of sphingomyelin to ceramide and phosphorylcholine. n-SMase2, a subfamily of sphingomyelinase, is associated with cellular stress response, ceramide-mediated apoptosis, inflammation, neurological disorders, small extracellular vesicle (sEV) biogenesis, and cancer development and metastasis [5-8]. During sEV biogenesis, a double membrane invagination of cell plasma membrane forms multivesicular bodies (MVB), which are either endosomal sorting complexes required for transport (ESCRT)-dependent or -independent process [31]. Therefore, n-SMase2 is a potential therapeutic target in different diseases where the biogenesis of sEVs is optional for using the ESCRT-independent pathway [32]. Inhibition of n-SMase2 presents a novel and selective antitumor strategy in PCa. This approach is particularly compelling given its broader implications for other diseases. For instance, in Parkinson's disease, the inhibition of n-SMase2 by cannabinol has been shown to reduce extracellular vesicle (EV) release and alpha-synuclein accumulation, leading to improved motor function in mice [33]. In another study, the inhibition of n-SMase2 by phenyl(*R*)-(1-(3-(3,4-dimetho-

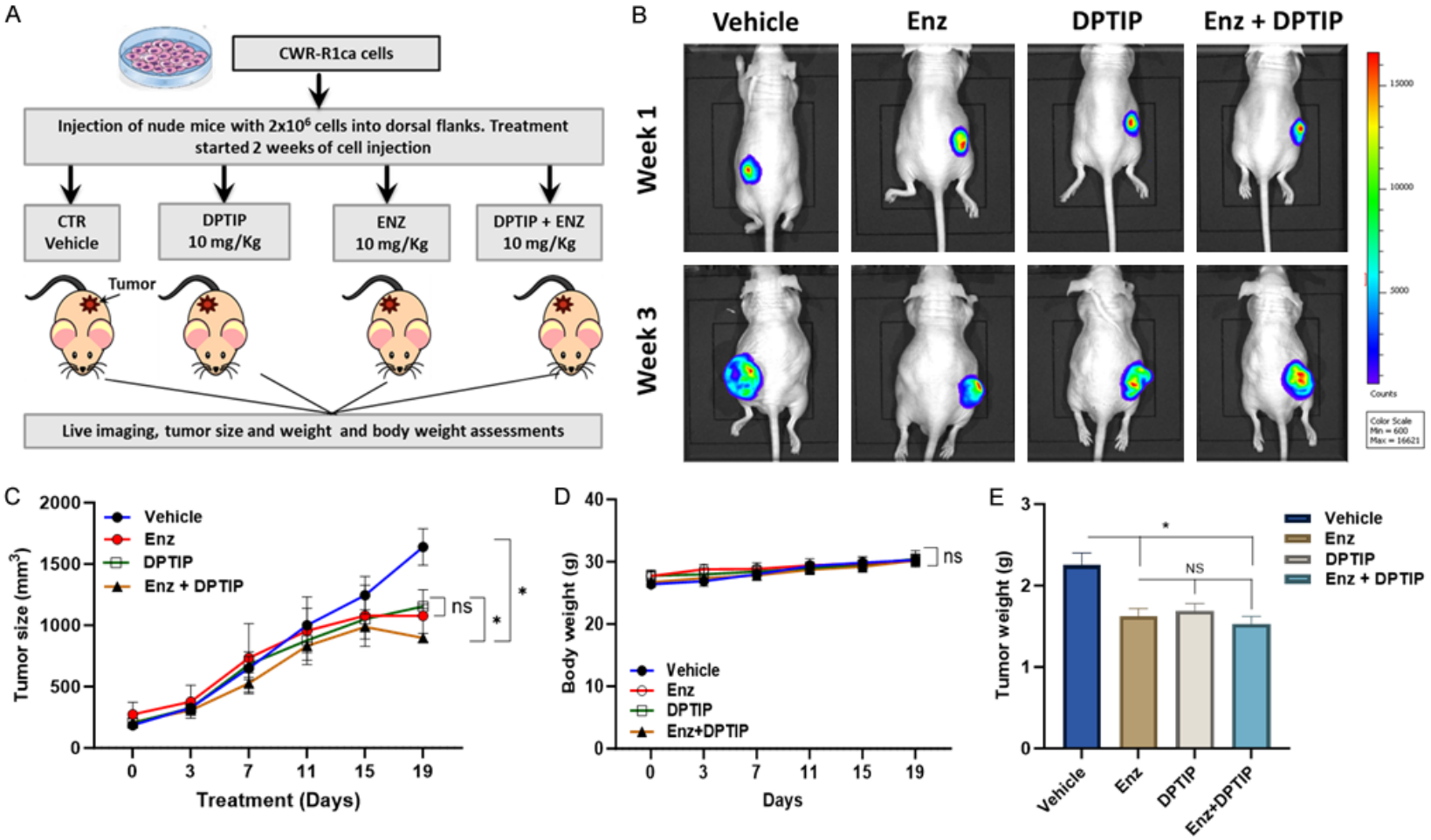

Figure 7. Antitumor effect of DPTIP in preclinical PCa model. (A) A representative experimental design for mice treatment. Mice were injected with CWR-R1ca-luc cells (2 × 10^6 cells). After 2 weeks, intraperitoneal injection of Enzalutamide (Enz) and DPTIP (10 mg/Kg each) was initiated and continued for another 3 weeks. (B) In Vivo Imaging was acquired at the baseline (week 1) and after 3 weeks of drug treatment. (C, D) Tumor size (C) and total body weight (D) were recorded twice a week for 3 weeks. (E) Tumor mass was excised after mice sacrifice and weighed. * depicts significance at $P<0.05$. NS: non-significant data.

xyphenyl)-2,6-dimethylimidazo[1,2-*b*]pyridazin-8-yl)pyrrolidin-3-yl) carbamate in neurons and oligodendrocytes decreased EVs secretion and activated microglia cells after acute brain injury [34]. DPTIP was reported to specifically inhibit n-SMase2 and suppress EV biogenesis, which reduces cytokine production in the liver and immune cell infiltration in the brain [9]. A research group developed an orally bioavailable and brain-penetrable prodrug called P18, which exerted 4-fold higher plasma and brain exposures versus the parent compound DPTIP [35]. These findings suggest the role of n-SMase2 in the pathogenesis of different diseases and justify the molecular targeting of n-SMase2 as an evidence-based approach for offering a new strategy for treating mCRPC patients.

Most FDA-approved drugs primarily target patients with localized CRPC and metastatic castration-sensitive PCa (mCSPC) [36]. The landscape for treating these conditions is continually evolving, with ongoing research aimed at improving outcomes for patients at various stages of the disease. Repurposing or developing novel drugs specifically targeting mCRPC remains an unmet clinical need. While ENZ exhibits variable efficacy depending on androgen receptor (AR) status in mCRPC cells, our findings demonstrate that DPTIP has a significant cytotoxic effect regardless of AR status. This suggests that DPTIP could be an effective treatment option across different subtypes of PCa, potentially overcoming some of the limitations associated with current therapies that are AR-dependent.

The consistent efficacy of DPTIP, as indicated by the recorded IC_{50} values across various PCa cells, underscores its potential as a promising candidate for further development in the treatment of mCRPC. This could pave the way for more effective therapeutic strategies that are less reliant on AR pathways, addressing a critical gap in the current treatment landscape. Interestingly, DPTIP showed a relative selectivity against PCa cells compared to normal PNT1A prostate epithelial cells. Therefore, the combination of DPTIP and ENZ could bring more benefits to mCRPC patients. The combination of ENZ with other therapeutic agents has been reported in different studies. For example, the combination of cholesterol-lowering simvastatin with the FDA-approved darolutamide inhibited CRPC cell growth *via* suppression of cell cycle regulators [37]. The treatment of CRPC cells with chemokine receptor CXCR7 inhibitor and ENZ suppressed cell growth and proangiogenic signaling pathways [38]. The combination of ENZ and sorafenib decreased cell proliferation-induced apoptosis *in vitro* and reduced tumor size in castration-resistant LNCaP-xenograft model [39]. It is well known that the aldo-keto reductase 1C3 (AKR1C3) enzyme is associated with intratumor androgen biosynthesis and development of CRPC status, and therefore, its pharmacological inhibition decreased cell growth and sensitized CRPC cells to ENZ [40]. Another research group used Akt pharmacological inhibitor AZD5363 in ENZ-resistant cells, and it reduced tumor size in the CRPC mouse model [41].

The combination treatment of mCRPC cells with both drugs at 0.5 IC_{50} significantly decreased the number of colonies and migratory cells compared to treatment with either drug alone. A group of researchers found that AR-positive PCa cells displayed sigmoidal dose-response curves for ENZ with IC_{50} values ranging from 19 to 45 μM as compared to AR-naïve cells, which had higher IC_{50} values [42]. This study is comparable with the IC_{50} values of ENZ-treated mCRPC cells recorded in our study. In an independent study, the inhibition of n-SMase2 by DPTIP downregulated mRNAs for a set of genes involved in transendothelial migration [43]. The same study showed that regulatory T cells inhibit n-SMase2 activity to prevent T-cell migration into intestinal tumors by decreasing chemokine secretion and vascular cell adhesion molecule 1 (VCAM1) expression. Exploring these gene targets may provide insights into the pathways affected by n-SMase2 inhibition and enhance our understanding of mCRPC behavior. Chemotherapeutic agents such as etoposide and paclitaxel activate n-SMase2 and induce cell apoptosis in PCa cells *via* protein kinase C delta (PKC-delta)-dependent pathway to mediate their cytotoxic effects [44]. In another study, Clarke *et al*. reported n-SMase2/S6K-axis as a significant component of all-trans-retinoic acid (ATRA)-induced cell cycle arrest in breast cancer cells [45]. When multiple myeloma and hepatocellular carcinoma cells were treated with n-SMase2 inhibitor cannabinol, the drug decreased cell

proliferation and induced cell apoptosis [46, 47]. When tissue-type plasminogen activator (tPA) activates smooth muscle cells and ECV-304 carcinoma cells, tPA promotes phosphorylation of ERK1/2 proteins through the sphingomyelin/ceramide pathway, which induces cell proliferation [48]. It was also reported that the blockade of the NF-kB pathway in cancer cells is associated with the inhibition of cell proliferation, migration, invasion, angiogenesis, drug resistance, and metastasis [49, 50]. Thus, the inhibition of these pathways by DPTIP aligns with the significant inhibition of cell growth, colony formation, and migration observed in mCRPC cells.

Our results demonstrate that the treatment of mCRPC cells leads to gene dysregulations associated with multiple signaling pathways. One notable example of a dysregulated gene is EXO5. The knockout of EXO5 in PCa cells impaired homology-directed recombination repair (HDR) and caused androgen-induced genomic instability [51]. The upregulation of EXO5 (14-fold) in our results suggests that DPTIP restored the tumor suppression function of this gene. It was reported that another dysregulated gene, fibulin-7 (Fbln7), inhibits tube formation [52]. These studies implicated the anti-angiogenic effect of Fbln7 in cancer, which aligned with our RNA-seq results (10-fold up). NKGA2 (KLRC1) is associated with improved survival and responsiveness to programmed death ligand 1 (PD-L1) blockade in bladder cancer with high $CD8^+$ T-cells [53]. The upregulation of fragile-site associated tumor suppressor (FATS or C10orf90) mRNA could be a prognostic marker for improved clinical outcomes in patients with non-small cell lung carcinoma (NSCLC) who received cisplatin-based chemotherapy [54, 55]. Another gene called Nox organizer 1 (NOXO1) belongs to the NADPH oxidase family and is associated with generating reactive oxygen species [56]. Long non-coding RNA LINC00482 inhibits tumor-associated inflammation and angiogenesis in bladder cancer and tumor metastasis in NSCLC [57, 58]. Our results show that NOXO1 and LINC00482 were downregulated after DPTIP treatment, which may validate their contribution to the n-SMase2 blockade. However, further studies are warranted to validate these genes in mCRPC cells.

The preclinical results show that mice treated with either DPTIP or ENZ revealed a significant reduction in tumor size. Notably, this effect was further enhanced when the two drugs were combined. Importantly, there were no observed effects on body weight, indicating that the combination treatment is well-tolerated. The research group that developed DPTIP reported that it exhibits potent non-competitive and selective inhibition against n-SMase2. Additionally, DPTIP has demonstrated metabolic stability in both mouse and human liver microsomes, indicating its potential for effective preclinical use without rapid degradation [9]. The inhibition of ceramide-S1P signaling with sphingosine kinase inhibitors enhanced ENZ efficacy in PCa cells through sterol regulatory element-binding protein 1 (SREBP)-induced lipotoxicity [59].

Although DPTIP has an excellent antitumor profile *in vitro*, the *in vivo* studies did not fully recapitulate the results observed in cell culture models. Several factors may contribute to this discrepancy, including drug pharmacokinetics, metabolic stability, and the need for dose adjustments [60]. These factors underscore the complexity of translating *in vitro* results to *in vivo* efficacy. In a study conducted on LNCaP-xenografted mice treated with ENZ at doses of 1, 10, and 50 mg/Kg daily, significant tumor size reduction was observed. Specifically, the 10 mg/kg dose resulted in a notable decrease in tumor size after 24 days of treatment, while the 50 mg/kg dose achieved similar results after 28 days [61].

One of the limitations of this study is that targeted downstream signaling pathways associated with the drug combination require further investigation. Additionally, the relatively short treatment duration in mice and the specific phenotype of prostate cancer (PCa) cells used in the study may limit the generalizability of the findings. Given the potential role of n-SMase2 in PCa, targeting this enzyme could represent a promising therapeutic strategy. Inhibiting n-SMase2 with DPTIP might not only suppress tumor growth and reduce metastasis but also enhance overall patient outcomes. However, more extensive research is needed to fully understand the complex role of n-SMase2 in mCRPC cells and to develop more effective therapeutic interventions. Future studies sh-

ould aim to explore the signaling pathways involved and evaluate different PCa models to strengthen the evidence for n-SMase2 as a viable therapeutic target.

Conclusions

Our study demonstrates that DPTIP exhibits potent anti-proliferative and anti-migratory effects on mCRPC cells *in vitro* and promotes tumor regression in a preclinical mouse model. Notably, the combination of DPTIP with ENZ proved to be more effective at reducing tumor size in CWR-R1Ca xenografts than either drug alone, suggesting a synergistic effect. These findings underscore the potential of DPTIP as a promising treatment candidate for mCRPC. Given the robust anti-tumor activity observed both *in vitro* and *in vivo* models, further preclinical studies and clinical investigations are warranted to explore its full therapeutic potential.

Acknowledgements

We thank Ms. Jennifer Arnold from VCOM's Grant Development Office for editing and proofreading the manuscript. RNseq was performed by the Tulane Center for Aging Genomics, Bioinformatics, and Spatial Multiomics Integrated Cores supported by NIH (P30GM-145498). This work was partially supported by the Delta Collaborative Research Program and VCOM REAP Funds (ZYA).

Disclosure of conflict of interest

None.

Address correspondence to: Dr. Zakaria Y Abd Elmageed, Department of Biomedical Sciences, Discipline of Pharmacology, Edward Via College of Osteopathic Medicine (VCOM), 4408 Bon Aire Drive, Monroe, LA 71203, USA. Tel: 318-342-7185; ORCID: 0000-0003-4031-0348; E-mail: zelmageed@ulm.vcom.edu

References

[1] Mirzaei S, Paskeh MDA, Okina E, Gholami MH, Hushmandi K, Hashemi M, Kalu A, Zarrabi A, Nabavi N, Rabiee N, Sharifi E, Karimi-Maleh H, Ashrafizadeh M, Kumar AP and Wang Y. Molecular landscape of LncRNAs in prostate cancer: a focus on pathways and therapeutic targets for intervention. J Exp Clin Cancer Res 2022; 41: 214.

[2] Buskin A, Singh P, Lorenz O, Robson C, Strand DW and Heer R. A review of prostate organogenesis and a role for iPSC-derived prostate organoids to study prostate development and disease. Int J Mol Sci 2021; 22: 13097.

[3] Sekhoacha M, Riet K, Motloung P, Gumenku L, Adegoke A and Mashele S. Prostate cancer review: genetics, diagnosis, treatment options, and alternative approaches. Molecules 2022; 27: 5730.

[4] Sharp A, Coleman I, Yuan W, Sprenger C, Dolling D, Rodrigues DN, Russo JW, Figueiredo I, Bertan C, Seed G, Riisnaes R, Uo T, Neeb A, Welti J, Morrissey C, Carreira S, Luo J, Nelson PS, Balk SP, True LD, de Bono JS and Plymate SR. Androgen receptor splice variant-7 expression emerges with castration resistance in prostate cancer. J Clin Invest 2019; 129: 192-208.

[5] Wu BX, Clarke CJ and Hannun YA. Mammalian neutral sphingomyelinases: regulation and roles in cell signaling responses. Neuromolecular Med 2010; 12: 320-330.

[6] Clarke CJ, Cloessner EA, Roddy PL and Hannun YA. Neutral sphingomyelinase 2 (nSMase2) is the primary neutral sphingomyelinase isoform activated by tumour necrosis factor-alpha in MCF-7 cells. Biochem J 2011; 435: 381-390.

[7] Kosaka N, Iguchi H, Hagiwara K, Yoshioka Y, Takeshita F and Ochiya T. Neutral sphingomyelinase 2 (nSMase2)-dependent exosomal transfer of angiogenic microRNAs regulate cancer cell metastasis. J Biol Chem 2013; 288: 10849-10859.

[8] Alessenko AV and Albi E. Exploring sphingolipid implications in neurodegeneration. Front Neurol 2020; 11: 437.

[9] Rojas C, Barnaeva E, Thomas AG, Hu X, Southall N, Marugan J, Chaudhuri AD, Yoo SW, Hin N, Stepanek O, Wu Y, Zimmermann SC, Gadiano AG, Tsukamoto T, Rais R, Haughey N, Ferrer M and Slusher BS. DPTIP, a newly identified potent brain penetrant neutral sphingomyelinase 2 inhibitor, regulates astrocyte-peripheral immune communication following brain inflammation. Sci Rep 2018; 8: 17715.

[10] Syvala H, Pennanen P, Blauer M, Tammela TL and Murtola TJ. Additive inhibitory effects of simvastatin and enzalutamide on androgen-sensitive LNCaP and VCaP prostate cancer cells. Biochem Biophys Res Commun 2016; 481: 46-50.

[11] Lopes N, Pacheco MB, Soares-Fernandes D, Correia MP, Camilo V, Henrique R and Jeronimo C. Hydralazine and enzalutamide: synergistic partners against prostate cancer. Biomedicines 2021; 9: 976.

[12] Schmidt KT, Chau CH, Strope JD, Huitema ADR, Sissung TM, Price DK and Figg WD. Anti-

tumor activity of NLG207 (formerly CRLX101) in combination with enzalutamide in preclinical prostate cancer models. Mol Cancer Ther 2021; 20: 915-924.
[13] Agarwal N, Azad AA, Carles J, Fay AP, Matsubara N, Heinrich D, Szczylik C, De Giorgi U, Young Joung J, Fong PCC, Voog E, Jones RJ, Shore ND, Dunshee C, Zschabitz S, Oldenburg J, Lin X, Healy CG, Di Santo N, Zohren F and Fizazi K. Talazoparib plus enzalutamide in men with first-line metastatic castration-resistant prostate cancer (TALAPRO-2): a randomised, placebo-controlled, phase 3 trial. Lancet 2023; 402: 291-303.
[14] Chandrashekar DS, Bashel B, Balasubramanya SAH, Creighton CJ, Ponce-Rodriguez I, Chakravarthi BVSK and Varambally S. UALCAN: a portal for facilitating tumor subgroup gene expression and survival analyses. Neoplasia 2017; 19: 649-658.
[15] Chandrashekar DS, Karthikeyan SK, Korla PK, Patel H, Shovon AR, Athar M, Netto GJ, Qin ZS, Kumar S, Manne U, Creighton CJ and Varambally S. UALCAN: an update to the integrated cancer data analysis platform. Neoplasia 2022; 25: 18-27.
[16] Cussenot O, Berthon P, Berger R, Mowszowicz I, Faille A, Hojman F, Teillac P, Le Duc A and Calvo F. Immortalization of human adult normal prostatic epithelial cells by liposomes containing large T-SV40 gene. J Urol 1991; 146: 881-886.
[17] Gaballah MSA, Ali HEA, Hassan ZA, Mahgoub S, Ali HI, Rhim JS, Zerfaoui M, El Sayed KA, Stephen D, Sylvester PW and Abd Elmageed ZY. Small extracellular vesicle-associated miR-6068 promotes aggressive phenotypes of prostate cancer through miR-6068/HIC2/SIRT1 axis. Am J Cancer Res 2022; 12: 4015-4027.
[18] Gaballa R, Ali HEA, Mahmoud MO, Rhim JS, Ali HI, Salem HF, Saleem M, Kandeil MA, Ambs S and Abd Elmageed ZY. Exosomes-mediated transfer of Itga2 promotes migration and invasion of prostate cancer cells by inducing epithelial-mesenchymal transition. Cancers (Basel) 2020; 12: 2300.
[19] Abd Elmageed ZY, Moroz K, Srivastav SK, Fang Z, Crawford BE, Moparty K, Thomas R and Abdel-Mageed AB. High circulating estrogens and selective expression of ERbeta in prostate tumors of Americans: implications for racial disparity of prostate cancer. Carcinogenesis 2013; 34: 2017-2023.
[20] Pandey RV, Pabinger S, Kriegner A and Weinhausel A. MutAid: sanger and NGS based integrated pipeline for mutation identification, validation and annotation in human molecular genetics. PLoS One 2016; 11: e0147697.
[21] Wang N, Reeves KJ, Brown HK, Fowles AC, Docherty FE, Ottewell PD, Croucher PI, Holen I and Eaton CL. The frequency of osteolytic bone metastasis is determined by conditions of the soil, not the number of seeds; evidence from in vivo models of breast and prostate cancer. J Exp Clin Cancer Res 2015; 34: 124.
[22] Wu J, Moverare-Skrtic S, Borjesson AE, Lagerquist MK, Sjogren K, Windahl SH, Koskela A, Grahnemo L, Islander U, Wilhelmson AS, Tivesten A, Tuukkanen J and Ohlsson C. Enzalutamide reduces the bone mass in the axial but not the appendicular skeleton in male mice. Endocrinology 2016; 157: 969-977.
[23] Ardiani A, Farsaci B, Rogers CJ, Protter A, Guo Z, King TH, Apelian D and Hodge JW. Combination therapy with a second-generation androgen receptor antagonist and a metastasis vaccine improves survival in a spontaneous prostate cancer model. Clin Cancer Res 2013; 19: 6205-6218.
[24] Abd Elmageed ZY, Yang Y, Thomas R, Ranjan M, Mondal D, Moroz K, Fang Z, Rezk BM, Moparty K, Sikka SC, Sartor O and Abdel-Mageed AB. Neoplastic reprogramming of patient-derived adipose stem cells by prostate cancer cell-associated exosomes. Stem Cells 2014; 32: 983-997.
[25] Yang Y, Jia D, Kim H, Abd Elmageed ZY, Datta A, Davis R, Srivastav S, Moroz K, Crawford BE, Moparty K, Thomas R, Hudson RS, Ambs S and Abdel-Mageed AB. Dysregulation of miR-212 promotes castration resistance through hnRNPH1-mediated regulation of AR and AR-V7: implications for racial disparity of prostate cancer. Clin Cancer Res 2016; 22: 1744-1756.
[26] Nickols NG, Nazarian R, Zhao SG, Tan V, Uzunangelov V, Xia Z, Baertsch R, Neeman E, Gao AC, Thomas GV, Howard L, De Hoedt AM, Stuart J, Goldstein T, Chi K, Gleave ME, Graff JN, Beer TM, Drake JM, Evans CP, Aggarwal R, Foye A, Feng FY, Small EJ, Aronson WJ, Freedland SJ, Witte ON, Huang J, Alumkal JJ, Reiter RE and Rettig MB. MEK-ERK signaling is a therapeutic target in metastatic castration resistant prostate cancer. Prostate Cancer Prostatic Dis 2019; 22: 531-538.
[27] Sparks JL, Kumar R, Singh M, Wold MS, Pandita TK and Burgers PM. Human exonuclease 5 is a novel sliding exonuclease required for genome stability. J Biol Chem 2012; 287: 42773-42783.
[28] Yamamoto T, Nakano H, Shiomi K, Wanibuchi K, Masui H, Takahashi T, Urano Y and Kamata T. Identification and characterization of a novel NADPH oxidase 1 (Nox1) inhibitor that suppresses proliferation of colon and stomach cancer cells. Biol Pharm Bull 2018; 41: 419-426.

[29] Ruiz C, Alborelli I, Manzo M, Calgua B, Keller EB, Vuaroqueaux V, Quagliata L, Rentsch CA, Spagnoli GC, Diener PA, Bubendorf L and Morant R; former members of the Urology Team in St. Gallen; Eppenberger-Castori S. Critical evaluation of transcripts and long noncoding RNA expression levels in prostate cancer following radical prostatectomy. Pathobiology 2023; 90: 400-408.

[30] Lin HM, Huynh K, Kohli M, Tan W, Azad AA, Yeung N, Mahon KL, Mak B, Sutherland PD, Shepherd A, Mellett N, Docanto M, Giles C, Centenera MM, Butler LM, Meikle PJ and Horvath LG. Aberrations in circulating ceramide levels are associated with poor clinical outcomes across localised and metastatic prostate cancer. Prostate Cancer Prostatic Dis 2021; 24: 860-870.

[31] Tkach M and Thery C. Communication by extracellular vesicles: where we are and where we need to go. Cell 2016; 164: 1226-1232.

[32] Tallon C, Hollinger KR, Pal A, Bell BJ, Rais R, Tsukamoto T, Witwer KW, Haughey NJ and Slusher BS. Nipping disease in the bud: nSMase2 inhibitors as therapeutics in extracellular vesicle-mediated diseases. Drug Discov Today 2021; 26: 1656-1668.

[33] Zhu C, Bilousova T, Focht S, Jun M, Elias CJ, Melnik M, Chandra S, Campagna J, Cohn W, Hatami A, Spilman P, Gylys KH and John V. Pharmacological inhibition of nSMase2 reduces brain exosome release and alpha-synuclein pathology in a Parkinson's disease model. Mol Brain 2021; 14: 70.

[34] Tallon C, Picciolini S, Yoo SW, Thomas AG, Pal A, Alt J, Carlomagno C, Gualerzi A, Rais R, Haughey NJ, Bedoni M and Slusher BS. Inhibition of neutral sphingomyelinase 2 reduces extracellular vesicle release from neurons, oligodendrocytes, and activated microglial cells following acute brain injury. Biochem Pharmacol 2021; 194: 114796.

[35] Pal A, Gori S, Yoo SW, Thomas AG, Wu Y, Friedman J, Tenora L, Bhasin H, Alt J, Haughey N, Slusher BS and Rais R. Discovery of orally bioavailable and brain-penetrable prodrugs of the potent nSMase2 inhibitor DPTIP. J Med Chem 2022; 65: 11111-11125.

[36] Meagher MF, Salmasi A and Stewart TF. Treatment landscape for metastatic castrate-sensitive prostate cancer: a review. Res Rep Urol 2023; 15: 509-517.

[37] Nakayama H, Sekine Y, Oka D, Miyazawa Y, Arai S, Koike H, Matsui H, Shibata Y and Suzuki K. Combination therapy with novel androgen receptor antagonists and statin for castration-resistant prostate cancer. Prostate 2022; 82: 314-322.

[38] Luo Y, Azad AK, Karanika S, Basourakos SP, Zuo X, Wang J, Yang L, Yang G, Korentzelos D, Yin J, Park S, Zhang P, Campbell JJ, Schall TJ, Cao G, Li L and Thompson TC. Enzalutamide and CXCR7 inhibitor combination treatment suppresses cell growth and angiogenic signaling in castration-resistant prostate cancer models. Int J Cancer 2018; 142: 2163-2174.

[39] Wu H, Zhang L, Gao X, Zhang X, Duan J, You L, Cheng Y, Bian J, Zhu Q and Yang Y. Combination of sorafenib and enzalutamide as a potential new approach for the treatment of castration-resistant prostate cancer. Cancer Lett 2017; 385: 108-116.

[40] Verma K, Gupta N, Zang T, Wangtrakluldee P, Srivastava SK, Penning TM and Trippier PC. AKR1C3 inhibitor KV-37 exhibits antineoplastic effects and potentiates enzalutamide in combination therapy in prostate adenocarcinoma cells. Mol Cancer Ther 2018; 17: 1833-1845.

[41] Toren P, Kim S, Cordonnier T, Crafter C, Davies BR, Fazli L, Gleave ME and Zoubeidi A. Combination AZD5363 with enzalutamide significantly delays enzalutamide-resistant prostate cancer in preclinical models. Eur Urol 2015; 67: 986-990.

[42] Haldrup J, Weiss S, Schmidt L and Sorensen KD. Investigation of enzalutamide, docetaxel, and cabazitaxel resistance in the castration resistant prostate cancer cell line C4 using genome-wide CRISPR/Cas9 screening. Sci Rep 2023; 13: 9043.

[43] Akeus P, Szeponik L, Langenes V, Karlsson V, Sundstrom P, Bexe-Lindskog E, Tallon C, Slusher BS and Quiding-Jarbrink M. Regulatory T cells reduce endothelial neutral sphingomyelinase 2 to prevent T-cell migration into tumors. Eur J Immunol 2021; 51: 2317-2329.

[44] Sumitomo M, Ohba M, Asakuma J, Asano T, Kuroki T, Asano T and Hayakawa M. Protein kinase Cdelta amplifies ceramide formation via mitochondrial signaling in prostate cancer cells. J Clin Invest 2002; 109: 827-836.

[45] Clarke CJ, Mediwala K, Jenkins RW, Sutton CA, Tholanikunnel BG and Hannun YA. Neutral sphingomyelinase-2 mediates growth arrest by retinoic acid through modulation of ribosomal S6 kinase. J Biol Chem 2011; 286: 21565-21576.

[46] Lu B, Zhang D, Wang X, Lin D, Chen Y and Xu X. Targeting SIRT1 to inhibit the proliferation of multiple myeloma cells. Oncol Lett 2021; 21: 306.

[47] Portmann S, Fahrner R, Lechleiter A, Keogh A, Overney S, Laemmle A, Mikami K, Montani M, Tschan MP, Candinas D and Stroka D. Antitumor effect of SIRT1 inhibition in human HCC

tumor models in vitro and in vivo. Mol Cancer Ther 2013; 12: 499-508.
[48] Maupas-Schwalm F, Auge N, Robinet C, Cambus JP, Parsons SJ, Salvayre R and Negre-Salvayre A. The sphingomyelin/ceramide pathway is involved in ERK1/2 phosphorylation, cell proliferation, and uPAR overexpression induced by tissue-type plasminogen activator. FASEB J 2004; 18: 1398-1400.
[49] Li B, Li YY, Tsao SW and Cheung AL. Targeting NF-kappaB signaling pathway suppresses tumor growth, angiogenesis, and metastasis of human esophageal cancer. Mol Cancer Ther 2009; 8: 2635-2644.
[50] Verzella D, Cornice J, Arboretto P, Vecchiotti D, Di Vito Nolfi M, Capece D, Zazzeroni F and Franzoso G. The NF-kappaB pharmacopeia: novel strategies to subdue an intractable target. Biomedicines 2022; 10: 2233.
[51] Ali S, Zhang Y, Zhou M, Li H, Jin W, Zheng L, Yu X, Stark JM, Weitzel JN and Shen B. Functional deficiency of DNA repair gene EX05 results in androgen-induced genomic instability and prostate tumorigenesis. Oncogene 2020; 39: 1246-1259.
[52] Ikeuchi T, de Vega S, Forcinito P, Doyle AD, Amaral J, Rodriguez IR, Arikawa-Hirasawa E and Yamada Y. Extracellular protein fibulin-7 and its C-Terminal fragment have in vivo anti-angiogenic activity. Sci Rep 2018; 8: 17654.
[53] Salome B, Sfakianos JP, Ranti D, Daza J, Bieber C, Charap A, Hammer C, Banchereau R, Farkas AM, Ruan DF, Izadmehr S, Geanon D, Kelly G, de Real RM, Lee B, Beaumont KG, Shroff S, Wang YA, Wang YC, Thin TH, Garcia-Barros M, Hegewisch-Solloa E, Mace EM, Wang L, O'Donnell T, Chowell D, Fernandez-Rodriguez R, Skobe M, Taylor N, Kim-Schulze S, Sebra RP, Palmer D, Clancy-Thompson E, Hammond S, Kamphorst AO, Malmberg KJ, Marcenaro E, Romero P, Brody R, Viard M, Yuki Y, Martin M, Carrington M, Mehrazin R, Wiklund P, Mellman I, Mariathasan S, Zhu J, Galsky MD, Bhardwaj N and Horowitz A. NKG2A and HLA-E define an alternative immune checkpoint axis in bladder cancer. Cancer Cell 2022; 40: 1027-1043, e1029.
[54] Song F, Zhang J, Qiu L, Zhao Y, Xing P, Lu J, Chen K and Li Z. A functional genetic variant in fragile-site gene FATS modulates the risk of breast cancer in triparous women. BMC Cancer 2015; 15: 559.
[55] Tian Y, Zhang J, Yan S, Qiu L and Li Z. FATS expression is associated with cisplatin sensitivity in non small cell lung cancer. Lung Cancer 2012; 76: 416-422.
[56] Moll F, Walter M, Rezende F, Helfinger V, Vasconez E, De Oliveira T, Greten FR, Olesch C, Weigert A, Radeke HH and Schroder K. Nox01 controls proliferation of colon epithelial cells. Front Immunol 2018; 9: 973.
[57] Xu W, Patel N, Deng Y, Ding S, Wang T and Zhang H. Extracellular vesicle-derived LINC00482 induces microglial M2 polarization to facilitate brain metastasis of NSCLC. Cancer Lett 2023; 561: 216146.
[58] Wang Y, Zhang L, Wei N, Sun Y, Pan W and Chen Y. Silencing LINC00482 inhibits tumor-associated inflammation and angiogenesis through down-regulation of MMP-15 via FOXA1 in bladder cancer. Aging (Albany NY) 2020; 13: 2264-2278.
[59] Lin HM, Mak B, Yeung N, Huynh K, Meikle TG, Mellett NA, Kwan EM, Fettke H, Tran B, Davis ID, Mahon KL, Zhang A, Stockler MR, Briscoe K, Marx G, Crumbaker M, Stricker PD, Du P, Yu J, Jia S, Scheinberg T, Fitzpatrick M, Bonnitcha P, Sullivan DR, Joshua AM, Azad AA, Butler LM, Meikle PJ and Horvath LG. Overcoming enzalutamide resistance in metastatic prostate cancer by targeting sphingosine kinase. EBioMedicine 2021; 72: 103625.
[60] Elwaie TA, Abbas SE, Aly EI, George RF, Ali H, Kraiouchkine N, Abdelwahed KS, Fandy TE, El Sayed KA, Abd Elmageed ZY and Ali HI. HER2 kinase-targeted breast cancer therapy: design, synthesis, and in vitro and in vivo evaluation of novel lapatinib congeners as selective and potent HER2 inhibitors with favorable metabolic stability. J Med Chem 2020; 63: 15906-15945.
[61] Guerrero J, Alfaro IE, Gomez F, Protter AA and Bernales S. Enzalutamide, an androgen receptor signaling inhibitor, induces tumor regression in a mouse model of castration-resistant prostate cancer. Prostate 2013; 73: 1291-1305.

Table S1. Clinical characteristics of PCa patients in TMA tissue slide

Variable	Normal	PCa
Total number	Hyperplasia: 7 Normal: 11	103
Age (Mean ± SD)	58.4 ± 20.8	68.5 ± 7.45
Gleason score (n)		
GS<7		20
GS=7		17
GS>7		60
Unknown		6
T-stage		
IIA		11
IIB		12
IIC		17
III		27
IV		15
Unknown		21
Lymph node (LN) involvement		
Yes		15
No		67
Unknown		21

Table S2. List of primer sequence used in the study

Gene	Description	Forward sequence	Reverse sequence
Exo5	Exonuclease 5	AGATGCCCAAGAGTCAAAGG	CCTTCTCAGGTGCCAAGAAA
FBLN7	Fibulin-7	CCAGATGCCCTTCCAGTTT	GGAGCATTCACTGATACCTCTAC
KLRC1	Killer Cell Lectin Like Receptor C1	AACCCAAAGAGGCAGCAA	GTTACCACAGAGGCCATTAAGA
C10orf90	Chromosome 10 Open Reading Frame 90	CTCACAAGAACGGCTGAAGA	GGCACGGAGTCTGTTACTTT
TBX4	T-box Transcription Factor 4	CCGACTGCAGAGCAAAGAATA	GCAGTGATAGAAGAGGCTTGAG
NOXO1	NADPH Oxidase Organizer 1	CGAATTCAGGCAGCTCAAGA	GTGCGAAGAAGCCAGTGAT
LINC00482	Long Intergenic Non-Protein Coding RNA 482	GATCATCCTTGGCGTCTGTT	CCTCAGAATGGGACCTTATTGG
GAPDH	Glyceraldehyde 3-Phosphate Dehydrogenase	GTCTCCTCTGACTTCAACAGCG	ACCACCCTGTTGCTGTAGCCAA

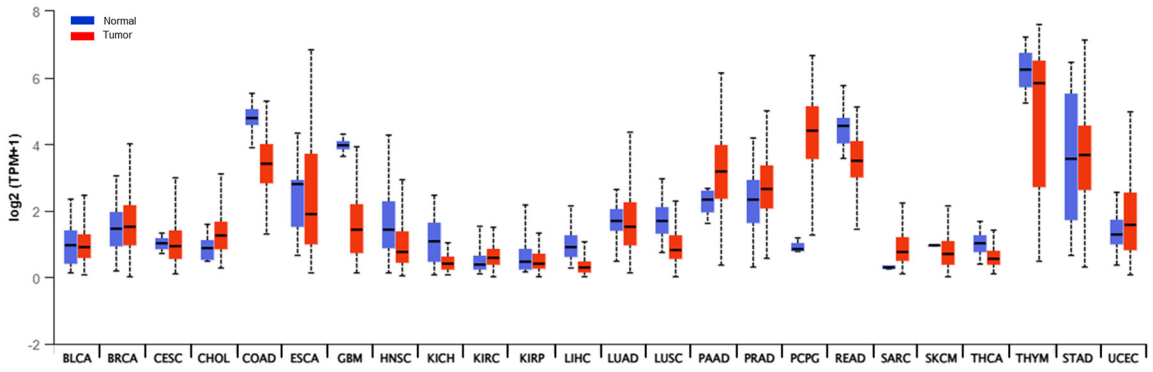

Figure S1. Expression of *SMPD3* gene in multiple types of cancers. TCGA data was analyzed by UALCAN website https://ualcan.path.uab.edu/ according to Chandrasekhar *et al.* (PMID: 28732212 & 35078134). *SMPD3* mRNA expression represented as log2 of transcripts per million (TPM). BLCA: Bladder urothelial carcinoma; BRCA: Breast invasive carcinoma; CESC: Cervical squamous cell carcinoma; CHOL: Cholangiocarcinoma; COAD: Colon adenocarcinoma; ESCA: Esophageal carcinoma; GBM: Glioblastoma multiforme; HNSC: Head and Neck squamous cell carci-

noma; KICH: Kidney chromophobe; KIRC: Kidney renal clear cell carcinoma; KIRP: Kidney renal papillary cell carcinoma; LIHC: Liver hepatocellular carcinoma; LUAD: Lung adenocarcinoma; LUSC: Lung squamous cell carcinoma; PAAD: Pancreatic adenocarcinoma; PRAD: Prostate adenocarcinoma; PCPG: Pheochromocytoma and paraganglioma; READ: Rectum adenocarcinoma; SARC: Sarcoma; SKCM: Skin cutaneous melanoma; THCA: Thyroid carcinoma; THYM: Thymoma; STAD: Stomach adenocarcinoma; UCEC: Uterine corpus endometrial carcinoma.

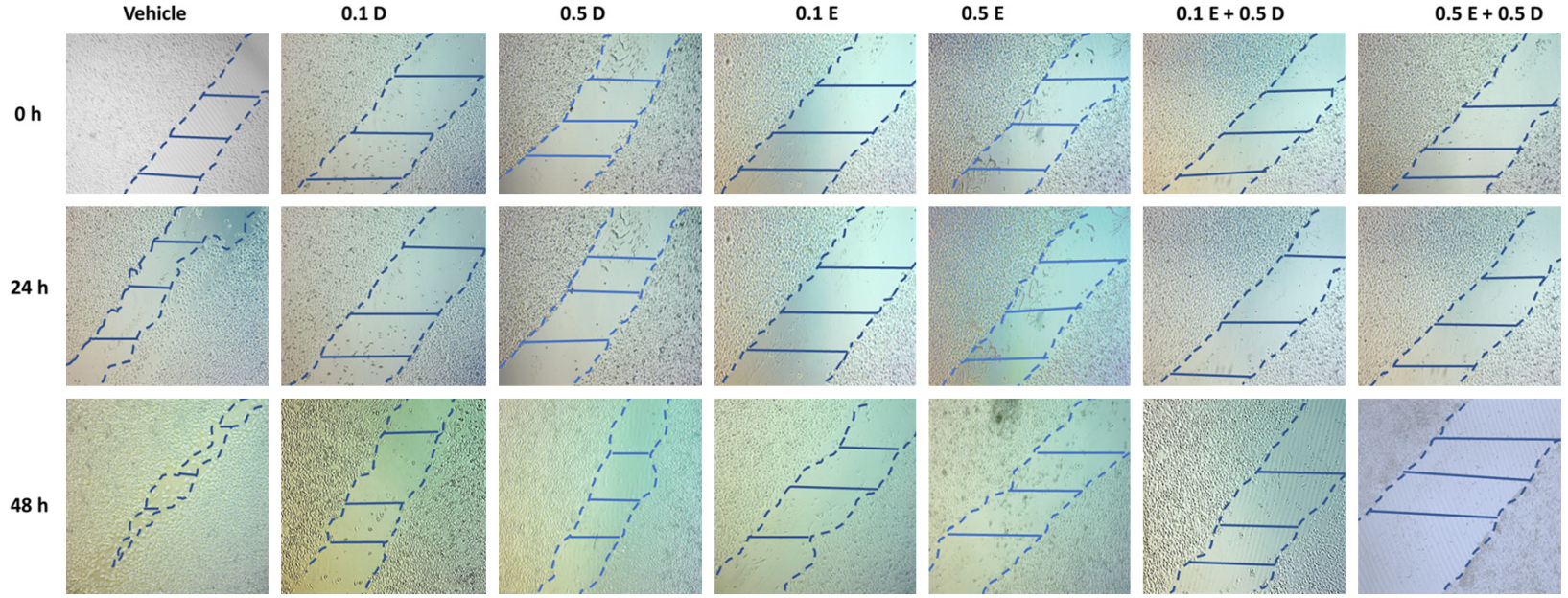

Figure S2. Wound-healing assay for treatment of PC-3 cells with DPTIP and Enzalutamide. Cells were seeded in 6-well plate till reach 80-90% confluency. Three scratches per well in duplicates were made and each well was treated with 0.1 and 0.5 IC_{50} of DPTIP and Enzalutamide. Each well was imaged at 0, 24 and 48 h of the treatment.

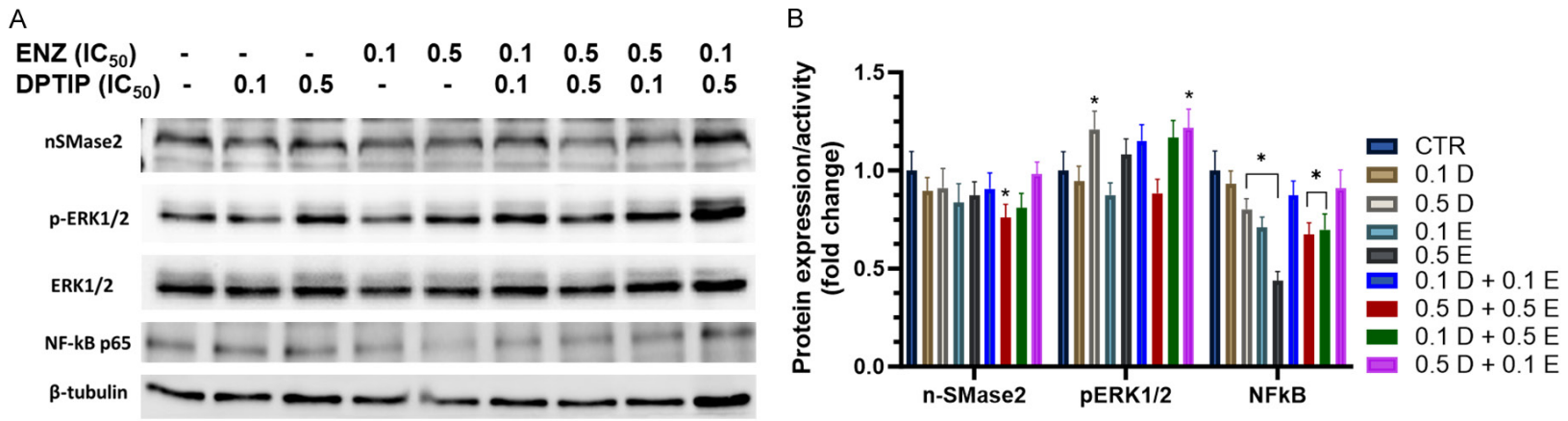

Figure S3. Molecular effect of DPTIP and Enzalutamide treatments on CWR-R1Ca cells. A. Cells were treated with 0.1 and 0.5 IC_{50} of DPTIP (D) and Enzalutamide (ENZ), and their combinations for 24 h. Cell lysates were resolved on gel and the membrane-bound proteins were incubated with antibodies against nSMase2, phosphorylated and total ERK1/2, and NF-kB p65. B. Relative expressions of nSMase2, phosphorylated ERK1/2 and NF-kB were calculated as fold change relative to beta-tubulin as a house keeping prtein. * depicts statistical significance at $P<0.05$ regarding vehicle control cells.